Disentanglement of the unoccupied electronic structure in metallic and semiconducting C_{60} peapods

C. Kramberger,[1] P. Ayala,[1] H. Shiozawa,[2] F. Simon,[1] A. Friedrich,[1] X. Liu,[1] M. Rümmeli,[3] Y. Miyata,[4] H. Kataura,[4] P. Hoffmann,[5] and T. Pichler[1]

[1]*Faculty of Physics, University of Vienna, Strudlhofgasse 4, A-1090, Vienna, Austria*
[2]*Advanced Technology Institute, University of Surrey, Guildford GU2 7XH, United Kingdom*
[3]*IFW Dresden, Helmholtzstraße 20, D-01069 Dresden, Germany*
[4]*Nanotechnology Research Institute, AIST, Tsukuba 305-8562, Japan*
[5]*BESSY, Albert-Einstein-Straße 15, D-12481 Berlin, Germany*

(Received 11 February 2011; revised manuscript received 12 April 2011; published 31 May 2011)

We provide insight into the C1s x-ray absorption response of C_{60} encaged in metallicity-sorted single-walled carbon nanotubes. The partial density of states observed for different constituent species unveils their distinct electronic properties. We identify the relative positions and filling of the one-dimensional van Hove singularities in the hosting nanotubes and the molecular orbitals of the encaged fullerenes. We directly address the possible charge transfer and especially the predicted existence of a shallow half-filled electronic t_{1u} band in metallic peapods. In the experiment, we find the t_{1u} of C_{60} unoccupied in the semiconducting nanotubes. In metallic nanotubes, it is observed 100–200 meV above the Fermi level E_F.

DOI: 10.1103/PhysRevB.83.195438 PACS number(s): 73.20.Mf, 73.22.−f, 78.20.Bh

I. INTRODUCTION

C_{60} peapods are an all-carbon compound consisting of single-walled carbon nanotubes (SWNTs) and encaged C_{60} fullerenes.[1,2] Their potential to tune the electronic properties of SWNTs has attracted attention. The electronic structures of C_{60} peapods have been intensively studied both theoretically[3–7] and experimentally.[8–10] On the one hand, Okada *et al.*[3,4] and Otani *et al.*[5] pointed out that the crossing of the t_{1u} band of C_{60} peas with the Fermi level, E_F, leads to a multicarrier state in the metallic C_{60} peapods. On the other hand, Dubay and Kresse[7] concluded that the t_{1u} band stays above E_F in the semiconducting peapods. Spectroscopic studies have also been performed by several groups.[2,8–14] Using C1s core-level excitation electron energy-loss spectroscopy (EELS), Liu *et al.*[9] demonstrated that the electronic and optical properties of C_{60} peas are very similar to those of C_{60} *fcc* fullerite. In that contribution, the authors concluded that the C_{60} states might only weakly hybridize with the SWNT states. In contrast, Hornbaker *et al.*[10] saw on a local scale in scanning tunneling spectroscopy (STS) a periodic spatial modification in the unoccupied states of peapods matching the C_{60} array, and concluded that the C_{60} states hybridize with the SWNT states. Investigations by Raman spectroscopy on the intercalation properties of C_{60} by Pichler *et al.*[8] showed that the lowest unoccupied molecular orbital (LUMO) t_{1u} of the C_{60} can be populated in *n*-type doping with K^+, but no electrons can be withdrawn from the highest occupied molecular orbital (HOMO) h_{1u} with $FeCl_3^-$. Shiozawa *et al.*[14] revealed and decomposed the occupied density of states by photoemission spectroscopy on an intrinsic mixture of semiconducting and metallic C_{60} peapods. The absence of t_{1u} was consistent with an energy above the Fermi level. Complementary to this, Rauf *et al.*[11] found in photoemission a prolonged Luttinger liquid in potassium intercalated peapods because the charge transfer goes first to the originally unoccupied t_{1u} and only then to the van Hove singularities (VHS) of the nanotubes. All these findings point at an unoccupied t_{1u} in metallicity mixed peapods, but they are missing any direct observation pinning down the actual binding energy.

The different predictions for the electronic behavior of both semiconducting and metallic peapods, as well as isolated experimental findings urge for bulk scale investigations on peapods consisting of C_{60} and metallicity-sorted SWNT. Here, we investigate the electronic properties of purely metallic and purely semiconducting peapods in comparison to the respective empty SWNT with unprecedented resolution using x-ray absorption (XAS). The individual features of the molecular orbitals of C_{60} are well resolved along with the VHS of the encapsulating nanotubes. We find that the onset of the C1s absorption edge in the metallic SWNT as well as the t_{1u} are, despite the theoretical predictions,[3,4] retained in the metallic peapods. Indeed, the spectroscopic findings corroborate an uniform electronic configuration with a distinct unoccupied t_{1u} orbital in the metallic and semiconducting peapods. Its binding energy lies 100–200 meV above E_F of the metallic SWNT.

II. EXPERIMENTAL

Two batches of metallicity-sorted SWNT material were used here. Batches I and II were synthesized by pulsed laser ablation. Batch I has a mean diameter and a standard deviation of $d_0 = 1.37$ nm, $\sigma = 0.08$ nm and batch II has $d_0 = 1.55$ nm, $\sigma = 0.23$ nm. Density gradient centrifugation[15] was applied to sort the metallicity for both batches.[16] Batch I was previously characterized by optical absorption spectroscopy (OAS) and XAS.[17,18] The synthesis as well as characterization by OAS and Raman spectrocopy of batch II is described by Rümmeli *et al.*[19,20].

Peapods were prepared as follows. First, the SWNTs were annealed at 350 °C under ambient atmosphere. Then, the SWNT and typically 5 mg of gold grade C_{60} from Sigma-Aldrich were sealed together in an evacuated (10^{-6} mbar) quartz ampoule. Filling with C_{60} was achieved by annealing the ampoules for 24 h at 650 °C. Excess C_{60} is removed by

subsequent annealing at 650 °C for 1 h in vacuum (10^{-6} mbar). The filling was checked by Raman spectroscopy using a LabRam HR800 single monochromator. The samples were excited with 1 mW at 488 nm.

XAS experiments were conducted at beamline UE52-PGM at BESSY II in Berlin. All samples were prior to measurements annealed in ultrahigh vacuum (5×10^{-9} mbar) at 600 °C in a preparation chamber to remove adsorbates. Higher temperatures would degrade the peapods or eventually form double wall carbon nanotubes. The samples were then *in situ* transferred to the measurement chamber and the XAS spectra were measured at 2×10^{-10} mbar. The resolving power of the plane grating monochromator is as good as 4×10^4.[21] XAS spectra were measured via bulk sensitive drain current, and the intrinsic spectra of the samples were obtained by dividing with the empty reference measured on freshly evaporated Au. Spectra are normalized to the edge jump behind the $\sigma^\star$ resonance.

III. RESULTS AND DISCUSSION

The successful preparation of peapods from the metallic and semiconducting SWNT is confirmed by the Raman spectra shown in Fig. 1. The A_{g2} mode of C_{60} is present in between the D and G lines of the nanotubes. Note, that the relative intensities of the lines in the metallic and semiconducting nanotubes are subject to different resonant Raman scattering cross sections.[22] The resonance condition for semiconducting ~1.4 nm SWNT implies off-resonance for the metallic nanotubes.[23] The relative intensity of the A_{g2} is boosted by a factor of ~25, due to the extra C_{60} inside the invisible majority of the metallic SWNT. The purity in density gradient metallicity-separated SWNT was determined with OAS to be ~95%.[16]

Resonant XAS at the C1s core level projects local electronic transitions into unoccupied states within atoms. Such excitations feature naturally electronic core holes. In bulk solids the latter lead to a narrowing and downshifting of the XAS response, whereas they are not prominent in

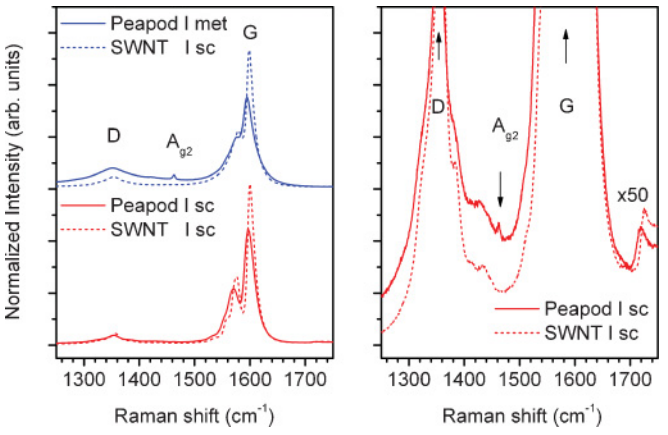

FIG. 1. (Color online) (Left panel) Raman spectra (488 nm) of the semiconducting (sc I) and metallic (met I) peapods and SWNT. The D and G bands are of the SWNT and the A_{g2} is a fingerprint of C_{60}. (Right panel) Enlargement of the Raman spectra of the semiconducting samples.

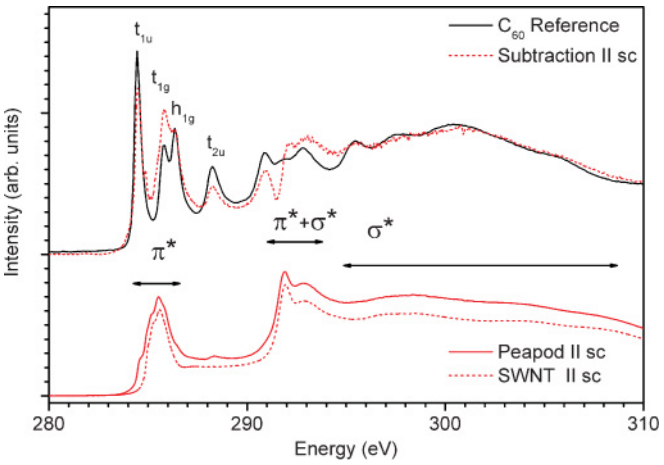

FIG. 2. (Color online) C1s XAS of the molecular resonances in C_{60} and the $\pi^\star$ and $\sigma^\star$ resonances of semiconducting (sc) peapods and SWNT from batch II. The dashed difference spectrum is obtained according to Eq. (1) with the best-fitting $c_m = 0.155$. The fit was performed in the denoted $\sigma^\star$ range. The SWNT spectrum is scaled with $1 - c_m = 0.845$, according to Table I

molecules.[24] Indeed, nanotubes offer as one-dimensional solids an intriguing composition of these flavors. The VHS peaks keep their original energy spacing of the band structure while the collective $\pi^\star$ response is contracted and downshifted. Therefore, the VHS are in the C1s XAS of nanotubes visible on top of the collective $\pi^\star$ resonance.[18,25,26]

The full C1s absorption edge of C_{60} fullerite, as well as semiconducting SWNT and peapods (batch II) can be seen in Fig. 2. The molecular response of C_{60} is visible in the compound response of the peapods. The peapod and nanotube spectra show the characteristic $\pi^\star$ and $\sigma^\star$ resonances of sp^2 carbon. The onset of the $\sigma^\star$ resonance is denoted as $\pi^\star + \sigma^\star$. C_{60} molecular orbitals are observed in the whole spectral range. The relative intensities of the molecular orbital in C_{60} are known to be subject to the local arrangement, whereas the total $\sigma^\star$ edge jump provides an uniform measure of its amount.[9,27] After normalization by the C1s $\sigma^\star$ edge jump, the C_{60} spectrum were reconstructed by subtracting the SWNT spectrum from the peapod spectrum, according to Eq. (1),

$$I_{C60} = \frac{1}{c_m}(I_{peapod} - (1 - c_m)I_{NT}), \qquad (1)$$

where c_m is the mass fraction of C_{60}. The obtained C_{60} pea spectrum, shown in Fig. 2, resembles the C_{60} reference spectrum and shows the t_{1u}, t_{1g}, h_{1g}, t_{2u} orbitals in the $\pi^\star$ range. The deviation in the $\pi^\star + \sigma^\star$ region is likely due to steep slopes in the original spectra. The $\sigma^\star$ region well above the C1s is fully reproduced in shape.

The right-hand panel of Fig. 3 shows the root mean square deviation of the simulated spectra to the fullerite reference. For both batches, the difference spectra were calculated according to Eq. (1). The root mean square deviation is integrated over the $\sigma^\star$ range (298–310 eV) and scaled by its total intensity. The so-determined mass contribution of C_{60} in the different peapods are shown in Table I next to the maximum possible mass contribution. To elaborate the

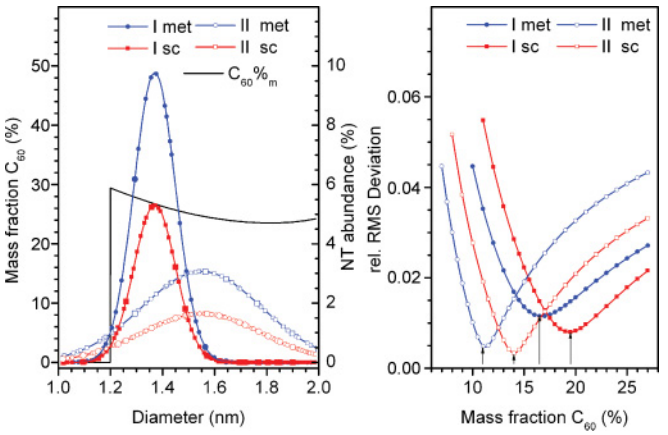

FIG. 3. (Color online) (Left panel) Overlay of the C_{60} mass fraction of completely filled peapods and the discrete Gaussian diameter distributions of batches I and II. The minimal diameter for filling is 1.2 nm and above $0.7 + (2 \times 0.335) = 1.37$ nm the 1-nm chain spacing is reduced due to zigzag arrangement (Ref. 28). Enlarged symbols show multiple chiralities per diameter. (Right panel) Relative root mean square (rel. rms) as evaluated for the $\sigma^\star$ resonance (298–310 eV) of both batches.

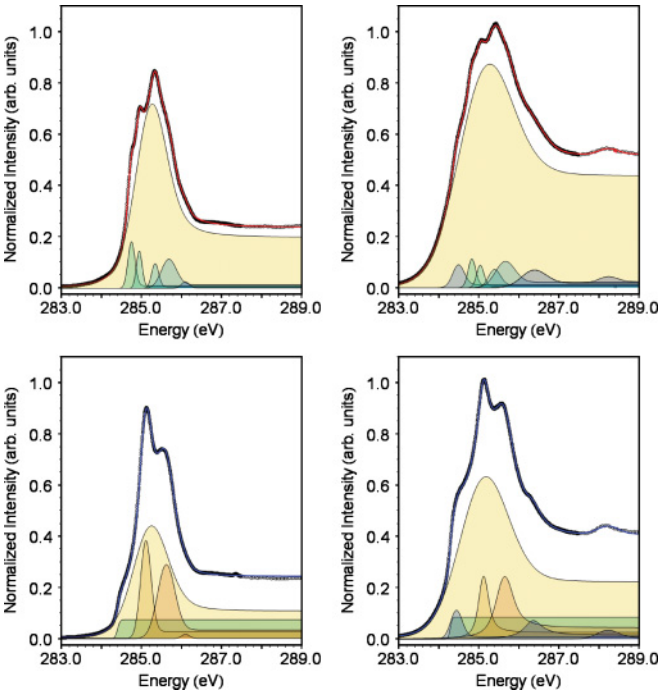

FIG. 4. (Color online) (Upper row) Lineshape analysis of the fine structures in the $\pi^\star$ XAS resonance of semiconducting SWNT I (left panel) and peapods I (right panel). (Lower row) Lineshape analysis for the metallic SWNT I (left panel) and peapods I (right panel).

latter, the discrete diameter distributions of batches I and II and the filling geometry of peapods are taken into account.[14,28] As illustrated in the left-hand panel of Fig. 3, both diameter distributions are well above the minimum required diameter. Note that the discrete diameters in the metallic SWNT are roughly twice as abundant because there are on average two semiconducting SWNT for every metallic SWNT. After an initial onset, the maximum possible C_{60} mass fraction is gradually decreased as the surrounding tube gets bigger than absolutely needed and above the best fitting diameter (1.37 nm), extra C_{60} can be accommodated in a zigzag configuration. The highest possible amount of C_{60} are found to be 26% in batch I and 24% in batch II. These limits are insensitive to either selecting only metallic or semiconducting SWNT. Table I reveals noteable differences in the achieved bulk filling among the samples. Since the exposure to C_{60} vapor has been thorough enough to ensure saturation, these differences are probably related to how effective and uniformly the preannealing process can create entrance sites for C_{60} in larger and smaller diameter or semiconducting and metallic SWNTs, respectively.

Note, that the t_{1u} LUMO of C_{60} peapods (see Fig. 2) manifests as a leading shoulder right at the onset of the $\pi^\star$ resonance. This finding concurs with the predictions of Dubay and Kresse[7] and reveals the previously hidden t_{1u} reported by Shiozawa *et al.*[14] The spectra also show that the t_{1u} is energetically below the first semiconducting VHS. These relative energies fully corroborate the studies on metallicity mixed and potassium intercalated peapods.[8,11,13] The comparison of doping behavior in SWNT and peapods allows to establish an energetic ordering of the LUMO, semiconducting VHS, and metallic VHS. The unequivocal conclusion in those studies is that the t_{1u} has the lowest binding energy and acts as a buffer accepting the donated electrons. Therefore the semiconducting and metallic VHS are in peapods only occupied at higher charge transfers than in SWNT. The present high resolution XAS spectra directly resolve the elusive t_{1u} in the conduction band of semiconducting and metallic peapods.

TABLE I. The mass fraction $C_{60}\%_m$ from the best fit is compared to the expected limit of ideal peapods shown in Fig. 3. The ratio of the latter two is the achieved filling $C_{60}\%_f$.

Batch	d_0 (nm)	σ (nm)	$C_{60}\%_m$	Limit $\%_m$	$C_{60}\%_f$
I met	1.37	0.08	16.5	26	63
I sc	1.37	0.08	19.5	26	74
II met	1.55	0.23	11.0	24	46
II sc	1.55	0.23	14.0	24	58

Figure 4 shows the lineshape analysis of the semiconducting and metallic SWNT and peapods from batch I. The semiconducting and metallic SWNT exhibit well-resolved peaks due to their respective VHS.[18] The metallic SWNT and peapods show additionally a metallic onset. The collective $\pi^\star$ resonance and fine structures due to VHS and molecular orbitals are fitted with Voigtian peaks. All peaks are modeled with an edge jump proportional to their area. The factor or proportionality is kept constant for all peaks in a spectrum.

The smaller diameters and significantly narrower diameter distribution in batch *I* exhibit better defined fine structures as compared to batch II. The higher resolution is partly diminished, but still superior, as the narrow tubes and the encapsulated C_{60} are under constant strain.[28]

The semiconducting nanotubes show from the left to the right a series of four finestructures $S_1^\star$–$S_4^\star$, which are also

TABLE II. Parameters of the lineshape analysis in Fig. 4. Edge jumps (step) are measured as percentage of peak areas. Peak areas and full width at half maxima (FWHM) are evaluated disregarding edge jumps.

Sample	Peak	Pos. (eV)	Area (%)	FWHM (meV)	Step (%)
SWNT I sc	$\pi^\star$	285.27	82.9	944	27.8
	$S_1^\star$	284.75	4.7	206	27.8
	$S_2^\star$	284.95	3.1	169	27.8
	$S_3^\star$	285.34	2.5	206	27.8
	$S_4^\star$	285.69	6.1	441	27.8
	–	286.10	0.8	238	27.8
Peapod I sc	$\pi^\star$	285.27	83.5	1601	38.9
	$S_1^\star$	284.82	1.9	223	38.9
	$S_2^\star$	285.03	1.5	212	38.9
	$S_3^\star$	285.42	1.9	352	38.9
	$S_4^\star$	285.69	4.3	572	38.9
	t_{1u}	284.47	2.3	343	38.9
	$t_{1g} + h_{1g}$	286.39	3.6	731	38.9
	t_{2u}	288.25	1.0	566	38.9
SWNT*I* met	$\pi^\star$	285.25	62.7	1046	29.5
	met	284.40	–	90	7.3[a]
	$M_1^\star$	285.11	16.7	309	29.5
	$M_2^\star$	285.62	20.1	507	29.5
	–	286.10	0.5	227	29.5
Peapod I met	$\pi^\star$	285.18	69.1	1444	26.6
	met	284.29	–	56	8.5[a]
	$M_1^\star$	285.12	8.0	298	26.5
	$M_2^\star$	285.65	13.4	521	26.5
	t_{1u}	284.44	3.3	338	26.5
	$t_{1g} + h_{1g}$	286.36	4.5	550	26.5
	t_{2u}	288.23	1.8	629	26.5

[a]Percentage of total $\pi + \sigma$ edge jump.

resolved in the peapod sample.[18] The $S_1^\star$–$S_4^\star$ peaks are notably suppressed in the peapods. In the metallic nanotubes, the $M_1^\star$ and $M_2^\star$ are identified, and they are also diminished in the peapod spectra.

In the semiconducting peapods, the $S_1^\star$–$S_4^\star$ are preceded by the t_{1u} and followed by the broadened and coalesced $t_{1g} + h_{1g}$ and the well-separated t_{2u} peaks of C_{60}. The positions, full width at half maxima (FWHM), areas and edge jumps of the aforedescribed peaks are summarized in Table II. The identification of the molecular orbitals as individual peaks in the $\pi^\star$ resonance of peapods proves unfilled and unperturbed molecular orbitals in the encaged C_{60}. In particular, the t_{1u} is also by quantitative line shape analysis reaffirmed as the LUMO in semiconducting peapods.[7]

In the metallic peapods, $M_1^\star$ and $M_2^\star$ are followed by the joined $t_{1g} + h_{1g}$ and the t_{2u}. Here, the t_{1u} is also observed as an independent molecular orbital. Its energy is above the metallic onset. This bulk scale finding is not in line with additional metallic channels as they where predicted in the metallic peapods.[3] The energies of the metallic onset and the t_{1u} are very close within the linewidths. We suggest that the proposed coupling mechanism between the encapsulated fullerenes via the metallic channel of the SWNT[3] may crucially rely on the ideal symmetry, which is not found in interwoven, curved, and statistically-filled real peapod material.

In semiconducting as well as metallic peapods, the distinctly observed molecular orbitals of C_{60} are fully consistent with an additive behavior without notable charge transfer in pristine peapods. In pristine peapods, the t_{1u} is 100–200 meV above the E_F. The well-defined uniformity across bulk samples of metallicity sorted peapods is an especially appealing aspect for employment in device architectures. The energies of 100–200 meV are easily accessible and open a window on electronic properties controllable via external fields and chemical modification.

IV. SUMMARY

We have prepared batches of the semiconducting and metallic C_{60} peapods. The successful preparation is confirmed by Raman spectroscopy and quantitatively evaluated from the edge jump in C1s core level XAS. High resolution XAS on the $\pi^\star$ resonance reveals uniform molecular orbitals inside the metallic and semiconducting peapods. The t_{1u} of C_{60} is in the semiconducting and metallic peapods likewise unoccupied. Its binding energy lies 100–200 meV above the Fermi level in the metallic SWNT. The uniformity of the t_{1u} derived states in bulk scale metallicity-sorted peapods shows the potential for defined performance in device architectures.

ACKNOWLEDGMENTS

C.K. acknowledges an APART fellowship 11456 of the Austrian Academy of Science. T.P. acknowledges DFG PI 440 4. P.A. acknowledges an individual Marie Curie Fellowship MEIF-CT2009-254125. F.S. acknowledges FWF P21333-N20. H.S. acknowledges the Leverhulme Trust for support through an early career fellowship. M.H.R. thanks the DFG RU1540/8-1.

[1]B. W. Smith, M. Monthioux, and D. E. Luzzi, Nature (London) **396**, 323 (1998).

[2]H. Kataura, Y. Maniwa, T. Kodama, K. Kikuchi, K. Hirahara, K. Suenaga, S. Iijima, S. Suzuki, Y. Achiba, and W. Kratschmer, Synth. Met. **121**, 1195 (2001).

[3]S. Okada, S. Saito, and A. Oshiyama, Phys. Rev. Lett. **86**, 3835 (2001).

[4]S. Okada, M. Otani, and A. Oshiyama, Phys. Rev. B **67**, 205411 (2003).

[5]M. Otani, S. Okada, and A. Oshiyama, Phys. Rev. B **68**, 125424 (2003).

[6]Y. Cho, S. Han, G. Kim, H. Lee, and J. Ihm, Phys. Rev. Lett. **90**, 106402 (2003).

[7]O. Dubay and G. Kresse, Phys. Rev. B **70**, 165424 (2004).

[8]T. Pichler, A. Kukovecz, H. Kuzmany, H. Kataura, and Y. Achiba, Phys. Rev. B **67**, 125416 (2003).

[9]X. Liu, T. Pichler, M. Knupfer, M. S. Golden, J. Fink, H. Kataura, Y. Achiba, K. Hirahara, and S. Iijima, Phys. Rev. B **65**, 045419 (2002).

[10]D. J. Hornbaker, S. J. Kahng, S. Misra, B. W. Smith, A. T. Johnson, E. J. Mele, D. E. Luzzi, and A. Yazdani, Science **295**, 828 (2002).
[11]H. Rauf, H. Shiozawa, T. Pichler, M. Knupfer, B. Buchner, and H. Kataura, Phys. Rev. B **72**, 245411 (2005).
[12]L. Kavan, L. Dunsch, and H. Kataura, Chem. Phys. Lett. **361**, 79 (2002).
[13]X. Liu, T. Pichler, M. Knupfer, J. Fink, and H. Kataura, Phys. Rev. B **69**, 075417 (2004).
[14]H. Shiozawa *et al.*, Phys. Rev. B **73**, 075406 (2006).
[15]M. S. Arnold, A. A. Green, J. F. Hulvat, S. I. Stupp, and M. C. Hersam, Nat. Nanotec. **1**, 60 (2006).
[16]Y. Sato, K. Yanagi, Y. Miyata, K. Suenaga, H. Kataura, and S. Lijima, Nano Lett. **8**, 3151 (2008).
[17]Y. Miyata, K. Yanagi, Y. Maniwa, and H. Kataura, J. Phys. Chem. C **112**, 13187 (2008).
[18]P. Ayala *et al.*, Phys. Rev. B **80**, 205427 (2009).
[19]M. H. Rummeli *et al.*, J. Phys. Chem. C **111**, 4094 (2007).
[20]M. H. Rummeli, C. Kramberger, M. Loffler, O. Jost, M. Bystrzejewski, A. Gruneis, T. Gemming, W. Pompe, B. Buchner, and T. Pichler, J. Phys. Chem. B **111**, 8234 (2007).
[21]A. Scholl, Y. Zou, T. Schmidt, R. Fink, and E. Umbach, J. Electron Spectrosc. Relat. Phenom. **129**, 1 (2003).
[22]H. Kuzmany *et al.*, Appl. Phys. A **76**, 449 (2003).
[23]H. Kataura, Y. Kumazawa, Y. Maniwa, I. Umezu, S. Suzuki, Y. Ohtsuka, and Y. Achiba, Synth. Met. **103**, 2555 (1999).
[24]O. Wessely, O. Eriksson, and M. I. Katsnelson, Phys. Rev. B **73**, 075402 (2006).
[25]C. Kramberger, H. Rauf, H. Shiozawa, M. Knupfer, B. Buchner, T. Pichler, D. Batchelor, and H. Kataura, Phys. Rev. B **75**, 235437 (2007).
[26]H. Shiozawa, T. Pichler, C. Kramberger, M. Rummeli, D. Batchelor, Z. Liu, K. Suenaga, H. Kataura, and S. R. P. Silva, Phys. Rev. Lett. **102**, 046804 (2009).
[27]M. Knupfer, Surf. Sci. Rep. **42**, 1 (2001).
[28]L. A. Girifalco, M. Hodak, and R. S. Lee, Phys. Rev. B **62**, 13104 (2000).